EBioMedicine 7 (2016) 135–145

Contents lists available at ScienceDirect

EBioMedicine

journal homepage: www.ebiomedicine.com

Research Paper

Low-Density Lipoprotein Receptor-Related Protein-1 Protects Against Hepatic Insulin Resistance and Hepatic Steatosis

Yinyuan Ding [a,b,h,i,1], Xunde Xian [a,b,*,1], William L. Holland [e], Shirling Tsai [f,g], Joachim Herz [a,b,c,d,**]

[a] Department of Molecular Genetics, UT Southwestern Medical Center, Dallas, TX 75390, USA
[b] Center for Translational Neurodegeneration Research, UT Southwestern Medical Center, Dallas, TX 75390, USA
[c] Department of Neuroscience, UT Southwestern Medical Center, Dallas, TX 75390, USA
[d] Department of Neurology and Neurotherapeutics, UT Southwestern Medical Center, Dallas, TX 75390, USA
[e] Department of Internal Medicine, Touchstone Diabetes Center, UT Southwestern Medical Center, Dallas, TX 75390, USA
[f] Department of Surgery, UT Southwestern Medical Center, Dallas, TX 75390, USA
[g] Dallas VA Medical Center, Dallas, TX 75216, USA
[h] Key Laboratory of Medical Electrophysiology, Ministry of Education of China, China
[i] Institute of Cardiovascular Research, Sichuan Medical University, Luzhou 646000, China

ARTICLE INFO

Article history:
Received 13 November 2015
Received in revised form 31 March 2016
Accepted 1 April 2016
Available online 4 April 2016

Keywords:
Insulin, metabolic syndrome
Insulin resistance
LRP1
Chylomicron remnant
Diabetes
Lipoprotein
PDGF

ABSTRACT

Low-density lipoprotein receptor-related protein-1 (LRP1) is a multifunctional uptake receptor for chylomicron remnants in the liver. In vascular smooth muscle cells LRP1 controls reverse cholesterol transport through platelet-derived growth factor receptor β (PDGFR-β) trafficking and tyrosine kinase activity. Here we show that LRP1 regulates hepatic energy homeostasis by integrating insulin signaling with lipid uptake and secretion. Somatic inactivation of LRP1 in the liver (hLRP1KO) predisposes to diet-induced insulin resistance with dyslipidemia and non-alcoholic hepatic steatosis. On a high-fat diet, hLRP1KO mice develop a severe Metabolic Syndrome secondary to hepatic insulin resistance, reduced expression of insulin receptors on the hepatocyte surface and decreased glucose transporter 2 (GLUT2) translocation. While LRP1 is also required for efficient cell surface insulin receptor expression in the absence of exogenous lipids, this latent state of insulin resistance is unmasked by exposure to fatty acids. This further impairs insulin receptor trafficking and results in increased hepatic lipogenesis, impaired fatty acid oxidation and reduced very low density lipoprotein (VLDL) triglyceride secretion.

1. Introduction

Low-density lipoprotein (LDL) receptor-related protein 1 (LRP1) is a multifunctional transmembrane receptor with diverse biological properties that are essential for the maintenance of normal mammalian physiology (Dieckmann et al., 2010). In the liver, LRP1 functions in concert with the LDL receptor (LDLR) in the clearance of ApoE-containing chylomicron remnants and very low density lipoprotein (VLDL) circulating in plasma (Rohlmann et al., 1998), as well as a number of other pro-atherogenic ligands (Espirito Santo et al., 2004). Hepatic LRP1 also binds hepatic lipase and lipoprotein lipase (LPL) (Verges et al., 2004), further contributing to the role of LRP1 in overall lipid homeostasis. In addition to functioning as an uptake receptor, LRP1 regulates intracellular trafficking of other cell surface receptors. In fibroblasts and smooth muscle cells, LRP1 controls platelet-derived growth factor receptor β (PDGFRβ) trafficking and tyrosine kinase activity, which in turn regulates extracellular signal regulated kinase (Erk) activation and cell proliferation. These mechanisms are fundamental to the protective role of LRP1 in atherogenesis and the protection of the vascular wall (Boucher et al., 2003; Takayama et al., 2005; Zhou et al., 2009).

The importance of LRP1 in lipid homeostasis and atherosclerosis is well established, however the role of LRP1 in glucose metabolism is just beginning to be understood. In vitro proteomic studies demonstrate that LRP1 functions as an integral component of glucose transporter storage vesicles (GSV) and LRP1 depletion in adipocytes is associated with decreased glucose transporter 4 (GLUT4) expression and decreased insulin-induced glucose uptake (Jedrychowski et al., 2010). In addition to regulating glucose uptake through GLUT4, LRP1 itself can be regulated by insulin signaling. In both adipocytes and hepatocytes, insulin stimulates a rapid translocation of LRP1 to the cell surface, leading to increased uptake of postprandial lipoproteins (Descamps et al., 1993; Laatsch et al., 2009). Moreover, a central role for LRP1 in overall energy metabolism is further suggested by a mouse model of induced LRP1 deficiency in the

* Correspondence to: X. Xian, Department of Molecular Genetics, UT Southwestern Medical Center, Dallas, TX 75390, USA.
** Correspondence to: J. Herz, Center for Translational Neurodegeneration Research, UT Southwestern Medical Center, Dallas, TX 75390, USA.
E-mail addresses: xunde.xian@utsouthwestern.edu (X. Xian), joachim.herz@utsouthwestern.edu (J. Herz).
[1] These authors contributed equally to this work.

http://dx.doi.org/10.1016/j.ebiom.2016.04.002

adult forebrain. This is associated with decreased leptin signaling, leading to accelerated weight gain and obesity, decreased energy consumption, and increased food intake (Liu et al., 2011).

Recently, the LIPGENE study has identified rs4759277 in the *Lrp1* gene as one of the top single nucleotide polymorphisms (SNPs) associated with fasting insulin levels and insulin resistance in patients with Metabolic Syndrome (Delgado-lista et al., 2014). Insulin resistance and dyslipidemia, in addition to central obesity, are key features of the Metabolic Syndrome. As a clinical entity, the prevalence of Metabolic Syndrome worldwide is increasing, largely related to rising rates of obesity and sedentary lifestyles (Grundy et al., 2005). The relationship between the hallmarks of the Metabolic Syndrome, in particular insulin resistance and dyslipidemia, is not well understood. However, it has been proposed that Metabolic Syndrome in general is mediated by an underlying insulin resistance (Grundy et al., 2004).

To explore the impact of LRP1 on insulin resistance and the Metabolic Syndrome, we generated a novel genetic model of diet-induced hepatic insulin resistance based on hepatic LRP1 deficiency. We found that liver-specific LRP1 knockout (hLRP1KO) mice when maintained on a standard chow diet exhibit mild dyslipidemia and impaired insulin signaling, however, when challenged with a high-fat diet (HFD) they rapidly develop obesity, marked insulin resistance, hyperglycemia, and hepatic steatosis. Collectively, these data suggest that hepatic LRP1 is essential for modulating hepatic insulin action and highlight a pivotal mechanism in the development of Metabolic Syndrome.

2. Materials and Methods

2.1. Materials

Human insulin was purchased from Humalog. The anti-phospho-insulin receptor (pIR), anti-IR, anti-protein kinase B (AKT), anti-pAKT, anti-β-actin, anti-glycogen synthase kinase (GSK) 3β, anti-pGSK3β and anti-calnexin antibodies were purchased from Cell Signaling. Anti-GLUT2 and anti-GLUT4 antibodies were purchased from Millipore. Anti-apolipoprotein B (apoB) and anti-apoE antibodies were purchased from Calbiochem. Generation of antibodies to LDLR, LRP1 and apoAI have been described previously (Ishibashi et al., 1993; Rohlmann et al., 1998). Peroxidase-labeled anti-rabbit or mouse IgG was from GH Healthcare and Peroxidase-labeled anti-goat IgG was from Santa Cruz. ECL system was from Thermo Scientific.

2.2. Mouse Experiments

Lrp1$^{flox/flox}$ mice were generated as previously described (Rohlmann et al., 1998; Rohlmann et al., 1996), and maintained on a mixed C57BL/6x 129SvJ strain background. Albumin-Cre mice on a congenic C57BL/6 background were from Jackson Laboratory (Stock number 003574). *Lrp1*$^{flox/flox}$ mice were crossed with albumin-Cre; *Lrp1*$^{flox/flox}$ mice to generate hLRP1KO and hLRP1$^{+/+}$ littermates (WT) by brother-sister mating. Animals were housed in specific pathogen-free facilities with 12-hour light/12-hour dark cycle. Animals were fed either a normal chow diet (Teklad 18%, Harlan) or a HFD containing 60% fat (D12492, Research Diets) ad libitum with free access to water. All experimental protocols were approved by the Institutional Animal Care and Use Committees of the University of Texas Southwestern Medical Center. Unless specifically mentioned, all experiments were performed on WT and hLRP1KO mice fed with chow or HFD for 16 weeks.

2.3. Glucose and Insulin Tolerance Tests

Glucose, insulin and pyruvate tolerance tests were performed 16 weeks after chow diet or HFD feeding; glucose tolerance test (1 g glucose/kg of body weight, after overnight fasting), insulin tolerance test (1 unit human regular insulin/kg body weight, after 6 h of fasting), and pyruvate tolerance test (1 g pyruvate/kg of body weight, after overnight fasting). Blood samples were obtained by tail bleeding and analyzed for glucose content (Contour brand glucometer) immediately before and at time points of 0, 30, 60, 90 and 120 min after an intraperitoneal injection.

2.4. Hyperinsulinemic Euglycemic Clamp

Anesthesia was accomplished by 2% isofluorane. For clamps, silicone catheters were aseptically placed in the jugular vein. Rimadyl (5 mg/kg, sc) was administered for pain control and animals were allowed to recover (4–5 days) to achieve preoperative weight prior to experiments. Clamps were performed in conscious unrestrained animals as previously described (Xia et al., 2015). Clamps were initiated by primed continuous infusion of insulin (3 mU/kg/min) and glucose was maintained constant at ~130 mg/dL during the clamped state.

2.5. In Vivo Insulin Stimulation

Following an overnight fast, mice were injected with 0.9% NaCl or 1 unit of regular human insulin/kg (Humalog) intraperitoneally. 5 min after injection of the insulin bolus, livers were rapidly removed and frozen in liquid nitrogen.

2.6. Primary Hepatocytes

Mouse primary hepatocytes were isolated from 8- to 10-week-old mice by collagenase perfusion as described previously (Wang et al., 2012). Cells were cultured in the presence of 1000 mg/L glucose and starved for overnight, following by 24-hour treatment with 0.25 mM albumin-bound Palmitate or 0.5% BSA. Insulin (100 nM/L) or 0.9% NaCl was added to the culture medium for 2 min.

2.7. Surface Protein Biotinylation

Primary mouse hepatocytes were grown in 6-well culture dishes and cell surface proteins were biotinylated as previously described (Chen et al., 2010). After insulin treatment, hepatocytes were washed with cold PBS buffer and then incubated in PBS buffer containing 1.0 mg/ml sulfo-NHS-SS-biotin (Pierce) for 30 min at 4 °C. Excess reagent was quenched by rinsing in cold PBS containing 100 mM glycine. Cell lysates were prepared in 160 μl of RIPA lysis buffer [50 mM Tris-HCl, 150 mM NaCl, 1% NP-40, 2 mM EDTA, 2 mM MgCl2, and protease inhibitor mixture (Sigma), (pH8.0)]. After 20 min incubated at 4 °C, lysates were collected and centrifuged at 14,000 × rpm for 10 min. 100 μg of total proteins were incubated with 100 μl of NeutrAvidin agarose (Pierce) at 4 °C for 1.5 h. Agarose pellets were washed three times using washing buffer [500 mM NaCl, 150 mM Tris-HCl, 0.5% Triton X-100 (pH8.0)], biotinylated surface proteins were eluted from agarose beads by boiling in 2x SDS sample loading buffer. Protein were separated by sodium dodecyl sulfate polyacrylamide gel electrophoresis (SDS-PAGE), transferred to nitrocellulose, and blotted with different antibodies.

2.8. Western Blot Analysis

Protein samples from liver tissues or hepatocytes were separated by SDS-PAGE and transferred onto nitrocellulose membranes (Bio-Rad). Blots were probed separately with antibodies as indicated in figures. After incubation with horseradish-peroxidase-conjugated secondary antibodies, membranes were visualized with SuperSignal West Pico Chemiluminescence reagents on X-ray films. When comparing phosphorylated and total IR and AKT protein, the same membranes incubated with phospho-antibodies were stripped and reprobed with non-phospho-antibodies. Band intensity was quantified using scanning densitometry of the autoradiogram with NIH Image J software (http://rsb.info.nih.gov/ij/).

2.9. Plasma and Liver Biological Parameter Analysis

After an overnight fast, animals were anesthetized with isoflurane and blood was collected. Total triglyceride (TG) and cholesterol were determined using a commercial kit (Infinity Triglyceride/Cholesterol Reagents, Thermo Scientific), and non-esterified fatty acid (NEFA) was assayed using commercial kits (Wako, Richmond, VA). Plasma from overnight-fasted mice was subjected to fast-performance liquid chromatography (FPLC) to assess the distribution of lipids within the lipoprotein fractions as described previously (Biddinger et al., 2008). For apolipoprotein analysis, equal volumes of whole plasma or pool of equal aliquots of three consecutive FPLC fractions were subjected to immunoblotting with apoB, apoE and apoAI antibodies. Plasma insulin was measured by using high sensitive mouse insulin enzyme-linked immunosorbent assay (ELISA) kit (Crystal Chem Inc.). Whole blood glucose was measured by blood glucose monitor (Contour). Hepatic lipids were extracted by homogenization of liver tissue (~100 mg) in chloroform:methanol at 2:1 by volume and analyzed as described (Ding et al., 2011).

2.10. VLDL Secretion Studies

To measure the VLDL-TG secretion rate, mice were fasted for 6 h, pre bled by retro orbital bleeding, and injected intravenously with 10% tyloxapol (Triton WR-1339; T-8761; Sigma-Aldrich, St. Louis, MO; 500 mg/kg body weight) to inhibit lipolysis. Plasma samples were drawn serially 0, 30, 60, 90 and 120 min after injection. Plasma TG from each time was measured by plate assay using Infinity TG Reagent (Thermo Scientific).

2.11. Histological Analysis

Livers were fixed by immersion in neutral buffered PFA (4%), and then transferred to OCT reagent for snap-freezing. 8-μm sections were stained with haematoxylin & eosin (H&E) or Oil O Red staining. Slides were analyzed using Zeiss Axiophot microscope and images captured with a SPOT digital camera.

2.12. Analysis of Gene Expression by Quantitative RT-PCR

Total RNA was isolated using RNeasy kit (Qiagen). Two microgram of RNA was reverse transcribed using random hexamer primers (Life technologies), and cDNA was diluted 1:20 and used for quantitative PCR employing gene-specific primers and SYBR Green reaction mix. Fluorescence was monitored and analyzed in an ABI prism 7900HT sequence detection system (Applied Biosystems). Each sample was measured in triplicate and the levels of each target mRNA were normalized to the levels of cyclophilin. Sequences of the primers used for real-time PCR were listed in Table S1.

2.13. Statistical Analysis

All data were expressed as mean ± SEM. Unpaired 2-tailed student's t test or two-way ANOVA test were used for statistical analysis. A P value of less than 0.05 between two groups was considered significant.

3. Results

3.1. Hepatic Inactivation of LRP1 in Mice Promotes Diet-induced Obesity

Hepatic LRP1 is essential for the uptake of chylomicron remnants by hepatocytes (Rohlmann et al., 1998). To investigate the effect of HFD in the setting of hepatic LRP1 deficiency, hLRP1KO mice were generated by breeding *Lrp1*$^{flox/flox}$ mice with albumin-Cre transgenic mice to yield hLRP1KO mice on a mixed C57BL/6x129SvJ background, as previously described (Basford et al., 2011; Rohlmann et al., 1996). Immunoblot analysis confirmed the deletion of LRP1 protein in liver from hLRP1KO mice, whereas LRP1 was preserved in the brain, white adipose tissue (WAT), and skeletal muscle (Fig. 1a). Eight-week-old male hLRP1KO mice and their littermate controls (*Lrp1*$^{flox/flox}$, or WT) were maintained on chow diet or HFD for 16 weeks. There was no difference in body weight between hLRP1KO and WT mice on chow diets. HFD resulted in increased body and fat mass in both WT and hLRP1KO mice, with hLRP1KO mice demonstrating significantly accelerated body weight gain starting at 14 weeks of age, leading to a 24.6% (50.98 ± 1.38 vs. 40.92 ± 1.47, $P < 0.01$) higher body weight when compared with WT mice at the end of the experiment. The dramatic weight gain was attributed entirely to an increase in body fat content and percent body fat (Fig. 1b and 1c). Metabolic measurements performed over a 5-day monitoring period showed no differences in daily food intake, O_2 consumption, CO_2 production, and total energy expenditure between WT and hLRP1KO mice on HFD (Fig. S1).

3.2. Liver LRP1 Deficiency Impairs Insulin Sensitivity and Aggravates Insulin Resistance in HFD-fed Mice

Obesity and increased adipocyte mass were suggestive of insulin resistance, as insulin is a key regulator in glucose and lipid metabolism. Therefore, we next investigated whether hLRP1 deficiency affected glucose homeostasis and insulin action. Although glucose and insulin concentrations in fasting plasma were not significantly different between WT and hLRP1KO mice on chow diet, HFD resulted in 73.9% higher plasma glucose (184.3 ± 16.02 vs. 106 ± 5.32, $P < 0.01$) and 60 % higher insulin (5.28 ± 0.37 vs. 3.3 ± 0.36, $P < 0.01$) levels in hLRP1KO mice than that observed in WT controls (Fig. 2a). To determine whole-body insulin sensitivity, we performed oral glucose tolerance tests (GTT), intraperitoneal insulin tolerance tests (ITT) and pyruvate tolerance tests (PTT) after dietary intervention for 16 weeks. Comparison of chow-fed WT and hLRP1KO mice demonstrated that these animals exhibited similar glucose tolerance, pyruvate tolerance and insulin sensitivity (Fig. 2b, 2c and 2d). In contrast, when compared with HFD-fed WT mice, the HFD-fed hLRP1KO mice displayed impaired glucose tolerance and pyruvate tolerance, associated with reduced insulin sensitivity ($P < 0.01$, Area Under Curve (AUC)), highlighting a loss of glycemic control.

To discern whether LRP1 deficiency or obesity was the primary trigger of impaired insulin action, we performed hyperinsulinemia-euglycemic clamp studies in 4-week HFD-fed mice, prior to any significant divergence in body weight (Fig. S2a). The glucose infusion rate required to maintain euglycemia trended lower in hLRP1KO mice (Fig. S2b), however, no changes in whole-body glucose turnover were apparent (Fig. S2c). Although endogenous glucose production was unchanged in the basal state (Fig. S2d, left panel), insulin suppressed hepatic glucose production much more effectively in WT mice (77.3 ± 12.9%) than hLRP1KO mice (26.4 ± 5.6%, $P < 0.005$) indicative of hepatic insulin resistance in hLRP1KO mice (Fig. S2d, right panel). Together, these data demonstrate that liver-specific disruption of the *Lrp*1 gene leads to latent hepatic insulin resistance, which can be unmasked by HFD.

3.3. Hepatic LRP1 Deficiency Impairs Insulin Signaling in the Liver

To better understand the mechanisms involved in insulin resistance in hLRP1KO mice, we investigated key insulin signaling molecules in livers from WT and hLRP1KO mice shortly after intraperitoneal injection of insulin. Immunoblotting of whole liver extracts revealed that tyrosine phosphorylation of IR, Serine473 phosphorylation of AKT, and Serine9 phosphorylation of GSK3β were markedly reduced in chow-fed and virtually absent in HFD-fed hLRP1KO mice compared with similarly treated WT controls (Fig. 3a and 3b). Furthermore, whereas interaction between insulin and IR normally inhibits gluconeogenesis, liver extracts from HFD-fed hLRP1KO mice showed a significant increase in glucose 6-phosphatase (*G6pc*) mRNA expression, a known gluconeogenic gene

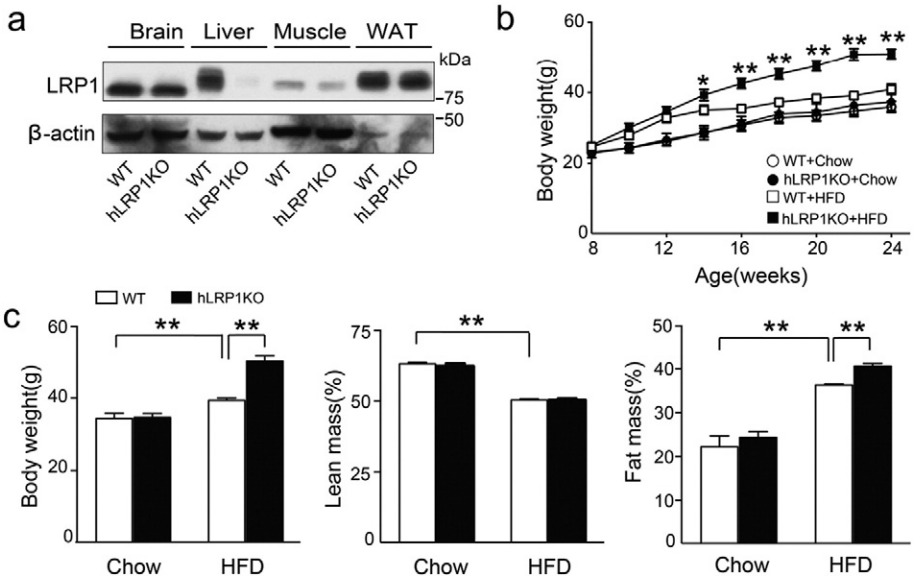

Fig. 1. Hepatic LRP1 deficiency promotes diet-Induced obesity. (a) Western blotting for LRP1 expression in tissue extracts prepared from brain, liver, skeletal muscle and white adipose tissue of WT and hLRP1KO mice. β-actin was used as loading control. (b) Body weight of age-matched male WT and hLRP1KO littermate mice that were fed chow diet or HFD for 16 weeks starting at 8 weeks of age. (n = 8–10 for each group, *P < 0.05; **P < 0.01 comparing hLRP1KO + HFD vs. WT + HFD). (c) Body weight and composition in 24-week-old WT and hLRP1KO mice after 16 weeks of chow diet or HFD (n = 6–10 per group, **P < 0.01).

(Fig. 3c). Interestingly, there was no change in the upstream component of the gluconeogenesis pathway, phosphoenolpyruvate carboxykinase 1(*Pck1*), suggesting that *G6pc* and *Pck1* are differentially regulated, as has been described (Muse et al., 2004). In light of this emerging picture of diet-induced insulin resistance, we wondered if there were also systemic manifestations of insulin resistance. Immunoblotting and immunohistochemistry of adipose tissue from hLRP1KO mice revealed inhibition of insulin-mediated AKT phosphorylation and adipocyte hypertrophy (Fig. S3, a, b and c). This is consistent with previous reports of increased plasma glucose levels leading to secondary adipocyte insulin-resistance. There were no corresponding differences in skeletal muscle (Fig. S3d). Together, these data suggest that hLRP1 deficiency leads to diet-induced hepatic and secondary adipocyte insulin resistance.

3.4. Hepatic LRP1 Deficiency Aggravates Palmitate-induced Insulin Resistance in Primary Hepatocytes

To verify the effect of HFD and hLRP1 deficiency on insulin resistance, primary hepatocytes from hLRP1KO and WT mice were treated with insulin (100 nM) after pre-incubation with either BSA or the saturated fatty acid palmitate. Consistent with in vivo results, we found a significant decrease in both phospho-IR and phospho-AKT in LRP1KO hepatocytes compared to WT hepatocytes under both BSA and palmitate treatment conditions (Fig. 4a and 4b).

To gain further insights into diet-induced insulin resistance in the context of hLRP1 deficiency, we investigated insulin-induced translocation of IR, LRP1 and GLUT2 in primary hepatocytes. Since receptor translocation is activated within a very short time frame, we first performed surface biotinylation at serial time points, which showed that receptor translocation was initiated starting at 2 min after treatment with insulin (Fig. S4). Therefore, we chose 2 min for our future surface biotinylation studies in vitro. As shown in Fig. 4c and 4d, in WT hepatocytes, insulin stimulates translocation of LRP1 to the plasma membrane, but this is inhibited by palmitate, suggesting that HFD alone can inhibit insulin-induced translocation of LRP1. Compared to WT hepatocytes, LRP1KO hepatocytes had decreased expression of surface IR (sIR), both at baseline (0.46 ± 0.09 vs. 1 ± 0.09, P < 0.05) and after stimulation with insulin (0.22 ± 0.16 vs. 0.5 ± 0.11). Treatment with palmitate diminished surface IR expression in WT cells, but LRP1KO cells still had lower IR expression at the plasma membrane. Importantly, however, insulin stimulated the internalization of IR to a similar extent in both WT and LRP1KO hepatocytes under BSA and palmitate-treated conditions. This suggests that LRP1 is necessary for efficient surface IR expression at the plasma membrane, but not for IR internalization in response to insulin.

In WT hepatocytes, insulin increased GLUT2 translocation in the presence of lipid-free BSA. In the presence of palmitate, surface GLUT2 expression was even higher, and was unresponsive to stimulation by insulin. However, GLUT2 translocation in LRP1KO hepatocytes did not respond to insulin either in the presence of BSA or palmitate. These findings suggest a model where diet-induced insulin-resistance in the hepatic LRP1 knockout is caused by attenuated surface expression of IR and impaired GLUT2 translocation, but insulin-dependent internalization of IR is unaffected.

Since the HFD consisted of 62% unsaturated fatty acids (~33% oleic, ~29% linoleic), we also examined whether these unsaturated fatty acid affected receptor translocation in vitro. Unlike plamitate, neither oleic nor linoic acids impaired insulin-stimulated LRP1 translocation in WT hepatocytes. However, both oleic and linoic acids had effects similar to that of palmitate on insulin-induced IR and GLUT2 translocation (Fig. S5 and S6). These results suggest that saturated and unsaturated fatty acids may differentially regulate receptor trafficking in hepatocytes.

3.5. Hepatic LRP1 Deficiency Leads to Diet-induced Dyslipidemia

Since hLRP1 is an essential regulator of lipoprotein metabolism, we next investigated the effect of hepatic LRP1 deficiency on plasma lipid levels in chow- and HFD-fed mice. As shown by Fig. 5a, on chow diet, compared with WT mice, hLRP1KO mice had a 2-fold increase in plasma TGs (185.4 ± 17.08 vs. 91.88 ± 7.66, P < 0.01), but on HFD, TGs were decreased by 37.5% (86.4 ± 2.91 vs. 138.2 ± 8.42, P < 0.01). FPLC lipoprotein analysis showed that this difference in plasma TG concentration was reflected by a corresponding decrease of VLDL levels (Fig. 5c). In terms of total cholesterol, on chow diet, hLRP1KO mice had significantly lower total plasma cholesterol levels (100.68 ± 3.75 vs. 123.09 ± 5.66, P < 0.01), as would be expected (Rohlmann et al., 1998), but this difference was abolished in mice on a HFD. FPLC lipoprotein analysis showed that cholesterol content in the HDL fractions in chow-fed hLRP1KO mice was significantly

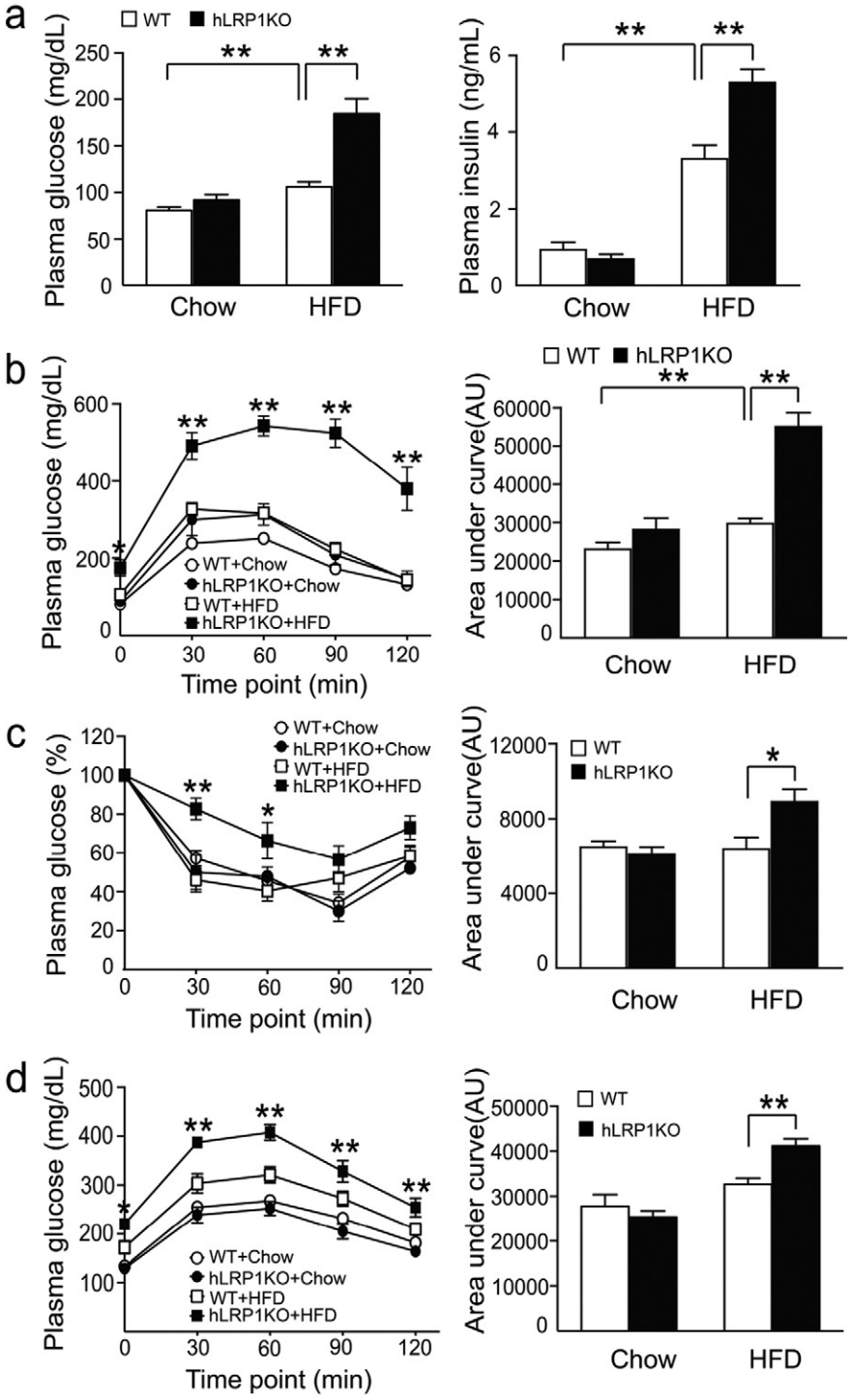

Fig. 2. LRP1 ablation aggravates diet-Induced insulin resistance. WT and hLRP1KO mice were maintained on chow diet or HFD for 16 weeks. (a) Fasting blood glucose and insulin levels (n = 9–17 for each group, *P < 0.05, **P < 0.01, mean ± SEM). (b) Glucose tolerance test. Blood glucose was measured at the indicated time points after oral administration of glucose (1 g/kg body weight). Area under the curve is quantified in the right panel (n = 9–11 for each group, *P < 0.05, **P < 0.01, mean ± SEM). AU, arbitrary unit. (c) Insulin tolerance test. Plasma glucose levels after intraperitoneal injection of insulin (1 IU/kg body weight), expressed as a percentage of basal glucose levels. Area under the curve is quantified in the right panel (n = 5–8 for each group, *P < 0.05, **P < 0.01, mean ± SEM). AU, arbitrary unit. (d) Pyruvate tolerance test. Plasma glucose levels after intraperitoneal injection of pyruvate (1 g/kg body weight). (n = 6–9 for each group, *P < 0.05, **P < 0.01, mean ± SEM). AU, arbitrary unit.

reduced compared to chow-fed WT mice, but there was no difference in cholesterol content of the HDL fraction in hLRP1KO and WT mice maintained on a HFD (Fig. 5c). Finally, chow-fed hLRP1KO mice exhibited significantly higher levels of circulating NEFA (1.76 ± 0.09 vs. 1.37 ± 0.09, P < 0.01). After HFD feeding, hLRP1KO mice still had increased NEFA levels compared to WT, but to a lesser extent (1.02 ± 0.03 vs. 0.91 ± 0.03, P < 0.05).

We then compared plasma apolipoprotein levels in WT and LRP1KO mice. Although LRP1 deficiency had no effect on plasma apoAI levels or distribution, apoB48 concentrations were markedly increased, with a shift toward smaller sizes of VLDL/LDL-containing fractions in hLRP1KO mice compared to WT mice on both chow and HFD (Fig. 5, b, c and d). On the other hand, apoE and apoB100 levels were significantly lower in hLRP1KO mice relative to controls when fed the chow

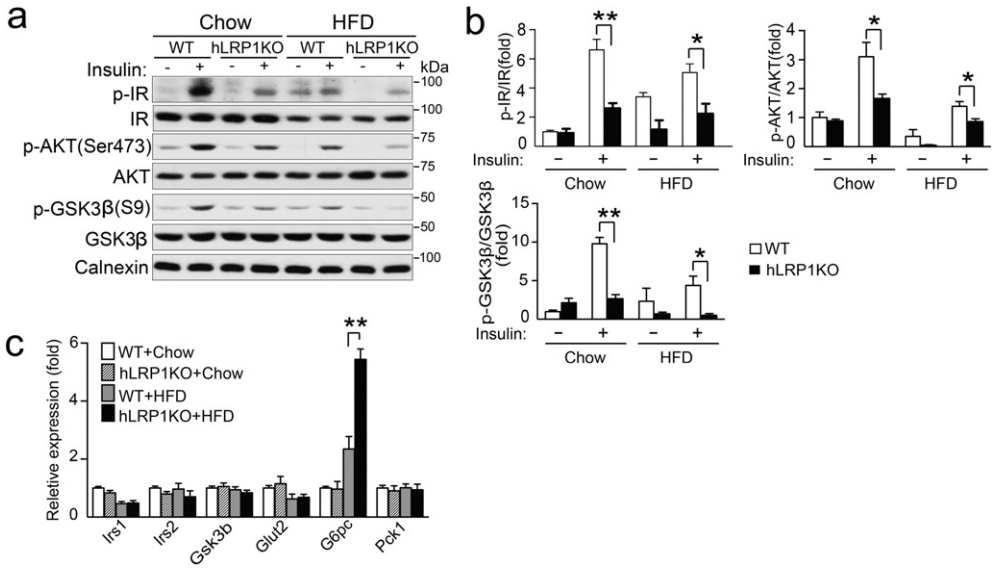

Fig. 3. Hepatic LRP1 deficiency impairs insulin signaling in liver. WT and hLRP1KO mice were maintained on chow diet or HFD for 16 weeks. (a) After overnight fast, mice were pre-treated with insulin (1 IU/kg, intraperitoneally), then sacrificed after 5 min. Total liver extracts were assayed for phosphorylation of IR, AKT and GSK3β, total IR, AKT and GSK3β expression by Western blot. Calnexin was used as loading control. (b) Densitometric quantification of the Western blot data (n = 4–5 for each group, *P < 0.05, **P < 0.01, mean ± SEM). (c) mRNA was extracted from the liver and subjected to quantitative PCR to assess expression of genes associated with insulin signaling, glucose transport and gluconeogenesis (n = 5 for each group, **P < 0.01, mean ± SEM).

diet, but these differences were abolished after HFD feeding. Given the altered lipid and apolipoprotein profile in hLRP1KO mice, we next measured VLDL-TG secretion and plasma apoB levels in WT and hLRP1KO mice by injecting tyloxapol to inhibit lipoprotein lipase activities. As shown in Fig. 6a and 6b, HFD in hLRP1KO mice resulted in impaired TG secretion. On the chow diet, the VLDL-TG secretion rate was 32.5% higher in hLRP1-KO mice than that in WT mice (7.29 ± 0.28 vs. 5.5 ± 0.31, P < 0.01). However, after HFD feeding, VLDL-TG secretion was 25.1% lower in hLRP1-KO mice when compared to WT mice (4.56 ± 0.29 vs. 6.1 ± 0.48, P < 0.05), and 37.4% lower when compared to baseline conditions (chow diet) (4.56 ± 0.29 vs. 7.29 ± 0.28, P < 0.01). In response to tyloxapol administration, WT apoB48 levels increased to a level comparable to those in hLRP1KO mice on chow diet, and on HFD, apoB48 levels in WT and hLRP1KO mice were indistinguishable (Fig. 6c and 6d). In contrast to apoB48, no changes in plasma apoB100 levels following tyloxapol treatment were observed in chow-fed or HFD-fed mice. Collectively, this variation in VLDL-TG secretion was not correlated with alterations of plasma apoB48 levels between WT and hLRP1KO mice, and enhanced plasma apoB48 in hLRP1KO mice mostly resulted from delayed clearance of plasma apoB48

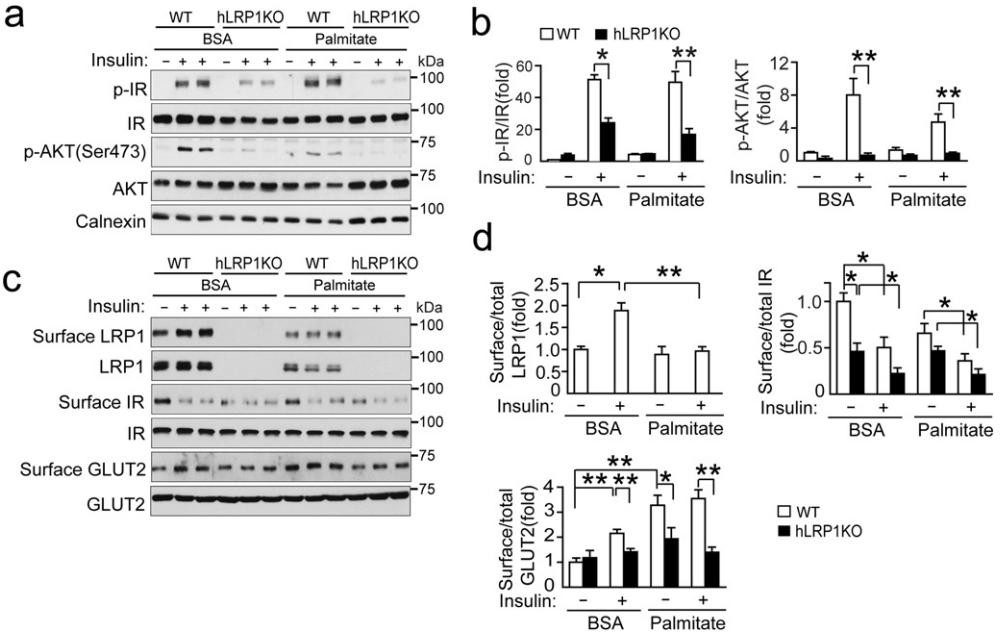

Fig. 4. LRP1 deficiency reduces insulin signaling and GLUT2 translocation in primary hepatocytes. Primary hepatocytes from WT and hLRP1KO mice were pre-incubated with 0.25 mM albumin-bound palmitate or 0.5% BSA for 24 h, followed by the treatment of 100 nM insulin for 2 min. (a) Representative Western blots for phosphorylated IR and AKT and total IR and AKT. Calnexin was used as loading control. (b) Densitometric quantification of the Western blot data. The results are representative of those obtained from three independent experiments (*P < 0.05, **P < 0.01, mean ± SEM). (c) Representative Western blots for surface biotinylated and total LRP1, IR, GLUT2. (d) Quantitative analysis of LRP1, IR, and GLUT2 translocation from three independent experiments (*P < 0.05, **P < 0.01, mean ± SEM).

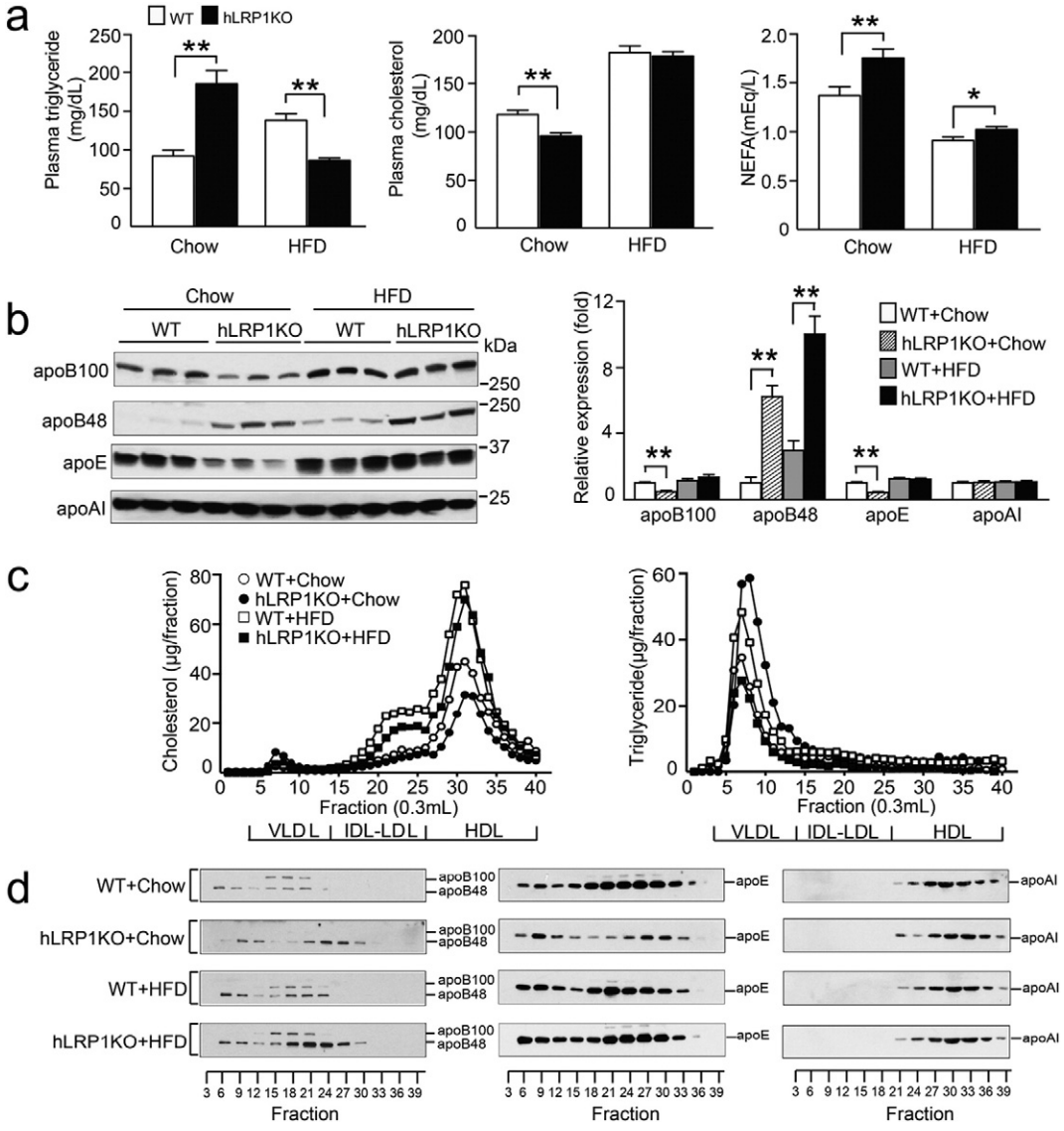

Fig. 5. Hepatic LRP1 deficiency leads to diet-Induced dyslipidemia. WT and hLRP1KO mice were maintained on 16 weeks of chow diet or HFD. Plasma was collected after overnight fast. (a) Plasma triglyceride, cholesterol and NEFA levels (n = 11–17 for each group, data are mean ± SEM, *P < 0.05; **P < 0.01). (b) Representative Western blot (left panel) and quantitative analysis (right panel) of plasma apolipoprotein levels (n = 5 for each group, data are mean ± SEM, **P < 0.01). (c) Pooled plasma from 5 mice from each group was analyzed by FPLC for lipoprotein cholesterol (left) and triglyceride (right) content. (d) Equal aliquots (0.3 mL) from three consecutive FPLC fractions were pooled for Western blot analysis of apoB100, apoB48, apoE and apoAI levels in the different fractions.

remnants rather than an increase of apoB48 secretion, consistent with the established role of LRP1 as a chylomicron remnant receptor.

3.6. Hepatic LRP1 Deficiency Promotes HFD-induced Hepatosteatosis

We next examined the pathophysiological consequences of abnormal lipoprotein metabolism in hLRP1KO mice. Morphological examination and Oil Red O staining of liver sections revealed a significant accumulation of lipid droplets in HFD-fed hLRP1KO mice compared to HFD-fed WT mice (Fig. 7a). This was reflected in a 33.1% increase in hepatic TG concentration (34.67 ± 0.64 vs. 26.05 ± 0.7, P < 0.01) and slightly higher (3.52 ± 0.54 vs. 3 ± 0.14, although not significantly) cholesterol content in hLRP1KO mice compared to WT mice on HFD (Fig. 7b). Although hLRP1KO mice showed a 45.5% higher hepatic NEFA content than WT mice after chow-feeding (0.024 ± 0.003 vs. 0.016 ± 0.002, P < 0.01), no difference of NEFA levels was detected in mice on HFD. Quantitative RT-PCR of RNA extracted from livers of WT and hLRP1KO mice on chow diet and HFD did not reveal any significant changes in the expression of inflammatory markers (Fig. S7). However, plasma levels of aspartate aminotransferase (AST) and alanine aminotransferase (ALT), were significantly higher in HFD-fed hLRP1KO mice (Fig. 7d). These findings are consistent with liver injury secondary to excess intrahepatic lipid accumulation, suggesting that hLRP1KO mice develop non-alcoholic hepatic steatosis after prolonged HFD. To gain insights into the molecular mechanisms underlying the hepatic steatosis associated with LRP1 deficiency in the liver, we analyzed genes involved in hepatic TG metabolism. As shown in Fig. 7c, the expression of most lipogenic genes, including those encoding fatty acid synthase (*Fas*), acetyl-CoA carboxylase (*Acc1*) and diacylglycerol acyltransferase (*Dgat1* and *Dgat2*), as well as the expression of hepatic genes relevant to lipid uptake (*Cd36*) and VLDL secretion (microsomal triglyceride transfer protein or *Mtp*), was similar between WT and hLRP1KO mice on chow or HFD. However, the expression of stearyl CoA desaturase 1 (*Scd1*) and glycerol-3-phosphate dehydrogenase (*Gpd1*) was significantly increased in both chow and HFD-fed hLRP1KO mice compared to WT mice. In addition, the expression of transcription factors involved hepatic lipogenesis, peroxisome proliferator-activated receptor gamma coactivator 1-alpha (*Ppargc1a*) and sterol regulatory

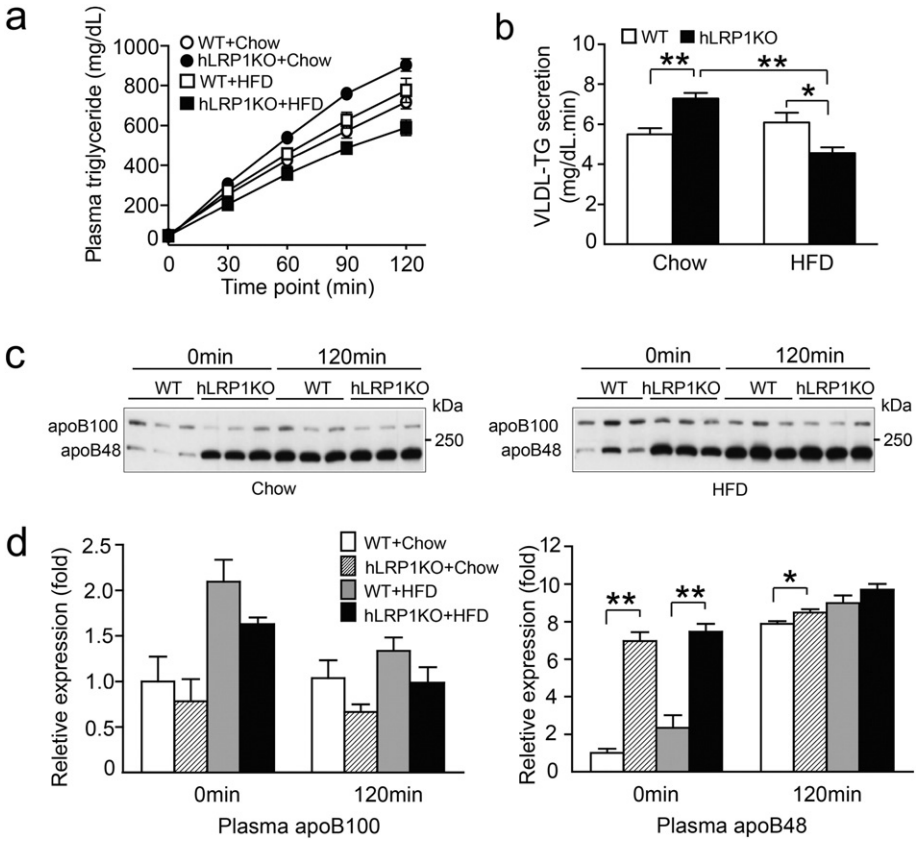

Fig. 6. HFD impairs hepatic VLDL-Triglyceride secretion in hLRP1KO mice. WT and hLRP1KO mice were maintained on chow diet or HFD for 16 weeks. After 6 h of fasting, mice were treated with an injection of tyloxapol. (a) Plasma VLDL-TG levels at the indicated time points after injection of tyloxapol (n = 5–7 for each group). (b) The rate of appearance of VLDL-TG in plasma was calculated from the slope of the graph in (a) (Data are mean ± SEM. *P < 0.05, **P < 0.01). (c) Western blot analysis of plasma apoB48 and apoB100 at the indicated time points after tyloxapol injection. (d) Quantitative analysis of plasma apoB48 and apoB100 from 3 independent Western blots (*P < 0.05, **P < 0.01, mean ± SEM).

element-binding factor-1c (*Srebf1c*) was significantly up-regulated, whereas the expression of acetyl-CoA oxidase (*Aco1*), an oxidoreductase involved in fatty acid metabolism, was significantly reduced in HFD-fed hLRP1KO mice. No change in the expression of MLX interacting protein-like (*Chrebp*), liver nuclear receptor subfamily 1 (*Lxra*), peroxisome proliferator-activated receptor alpha (*Ppara*) and peroxisome proliferator-activated receptor gamma (*Pparg*) was observed (Fig. S8). Together, the changes in gene expression profile suggest that LRP1 deficiency, combined with an excess of fatty acids, results in a pathological shift of hepatic fatty acid metabolism from an oxidative to a synthetic state.

In summary, our data demonstrate that hepatic LRP1 deficiency causes a latent insulin-resistance, due to disrupted trafficking of IR and GLUT2, which is unmasked by HFD. The resulting dyslipidemia is associated with impaired hepatic TG secretion and a shift in fatty acid metabolism towards fatty acid synthesis, leading to increased intrahepatic lipid accumulation and ultimately liver injury associated with hepatic steatosis.

4. Discussion

Our present studies in hLRP1KO mice show that hepatic inactivation of LRP1 primarily impairs insulin signal transduction by reducing surface IR expression and suppressing GLUT2 translocation to plasma membrane under normal physiological conditions. On a HFD, hLRPKO mice develop severe insulin resistance and obesity. As a consequence of nearly complete loss of hepatic insulin action, hLRP1KO mice develop dyslipidemia secondary to increased lipogenesis, reduced fatty acid oxidation and reduced VLDL secretion. Collectively, our current results demonstrate that hepatic LRP1 is a key regulator of insulin signaling and lipid homeostasis, two mechanisms that contribute to Metabolic Syndrome.

A growing body of evidence has shown that excess dietary fat intake impairs insulin action and leads to selective insulin resistance in the liver (Perry et al., 2014; Riccardi et al., 2004) where LRP1 is abundantly expressed and participates in lipoprotein metabolism (Rohlmann et al., 1998). However, the physiological impact of hepatic LRP1 in selective insulin resistance has remained elusive, thus prompting us to investigate the relationship between LRP1 and hepatic insulin resistance. Although no any obvious phenotype of insulin resistance was observed in chow-fed hLRP1KO mice, our hyperinsulinemic-euglycemic clamp studies indicate that targeted deletion of LRP1 is the primary cause of hepatic insulin resistance, indicating that hepatic LRP1 is a critical determinant of insulin sensitivity and hepatic insulin signal transduction. When hLRP1KO mice were challenged with an HFD, they developed whole-body insulin resistance characterized by hyperinsulinemia, mild fasting hyperglycemia and glucose intolerance. Accordingly, LRP1 deficient livers fail to respond to hyperinsulinemia, as evidenced by incomplete suppression of hepatic gluconeogenic genes and impaired insulin-induced phosphorylation of IR, AKT and GSK3β. These findings are consistent with the general consensus that enhanced gluconeogenesis, secondary to impaired insulin action in hepatocytes, is a leading cause of fasting hyperglycemia in Metabolic Syndrome. The blunted activation of Akt and its downstream effector GSK3β in response to insulin can be attributed to decreased expression of surface IR. Our findings in primary hepatocytes are consistent with in vitro results demonstrating that insulin stimulates the translocation of intracellular LRP1 to the plasma membrane in different cell types (Descamps et al., 1993; Laatsch et al., 2009; Liu et al., 2015), a process that is accompanied by the rapid internalization of surface IR. Strikingly, however, insulin-induced

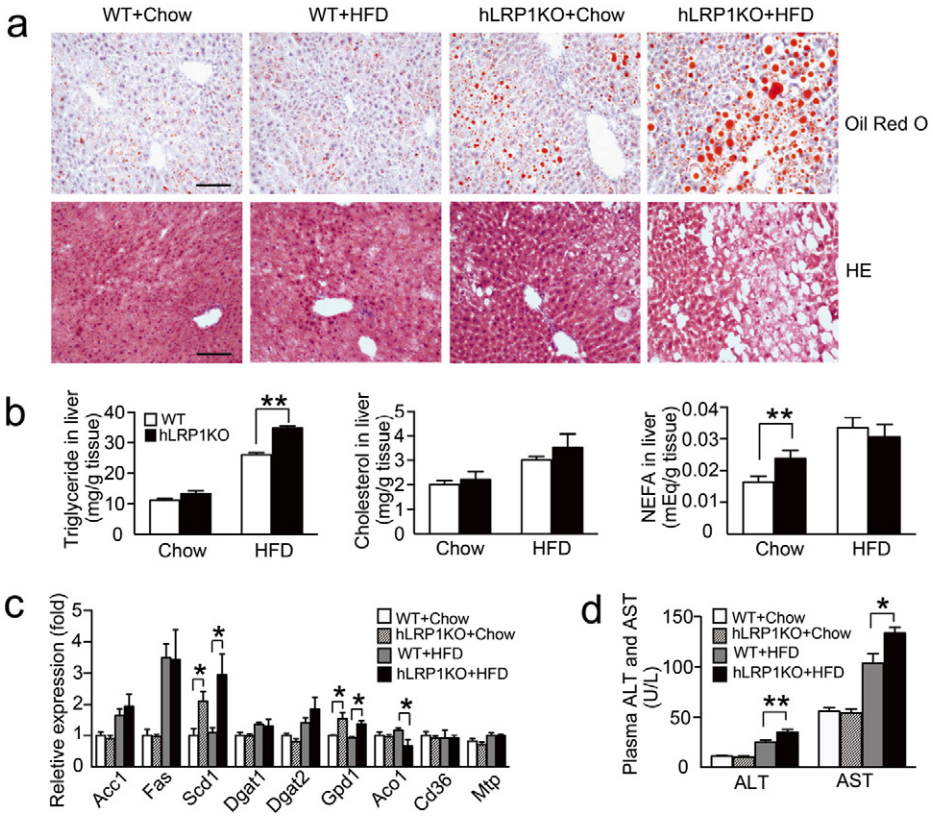

Fig. 7. Hepatic deletion of LRP1 accelerates the development of diet-induced fatty liver. (a) Representative Oil Red O staining (upper panel) and haematoxylin & eosin staining (lower panel) of liver from WT and hLRP1KO mice on chow diet or HFD for 16 weeks. Scale bar = 100 μm. (b) Lipids were extracted from the liver of WT and hLRP1KO mice maintained on chow diet and HFD. Hepatic TG, total cholesterol and NEFA content were determined (n = 5 for each group, $^{**}P < 0.01$, mean ± SEM). (c) Expression of key genes involved in fatty acid metabolism and lipogenesis was evaluated by real-time PCR of reverse transcribed cDNA extracted from the livers of WT and hLRP1KO mice (n = 5 for each group, $^{*}P < 0.05$, $^{**}P < 0.01$, mean ± SEM). (d) Plasma ALT and AST concentrations from WT and hLRP1KO mice after 16 weeks of chow diet or HFD (n = 5–8 for each group, $^{*}P < 0.05$, $^{**}P < 0.01$, mean ± SEM).

translocation of LRP1 is markedly attenuated in the presence of the free fatty acid palmitate. An association between LRP1 and IR is supported by a recent proteomic analysis demonstrating the presence of a LRP1-insulin receptor complex that functions in a co-internalization process for insulin clearance in mouse liver (Bilodeau et al., 2010). Unexpectedly, although LRP1KO hepatocytes have decreased surface IR expression, there was no change in insulin-stimulated internalization of IR, indicating that unlike in primary neurons (Liu et al., 2015), there may be other mechanisms that govern IR internalization in the liver. Because insulin-activated IR internalization remains intact in LRP1KO hepatocytes, interaction of IR with LRP1 primarily controls IR expression at the plasma membrane, but not its endocytosis.

LRP1 may also act as an essential scaffolding molecule that facilitates insulin-stimulated tyrosine phosphorylation of IR and downstream signaling cascades. Loss of LRP1 translocation, or attenuated LRP1 translocation in the presence of palmitate, would then result in impaired hepatic insulin signaling.

In addition to regulating surface IR expression, LRP1 is a key component of GSVs that regulate GLUT4 trafficking (Jedrychowski et al., 2010). Depletion of LRP1 from 3T3-L1 adipocytes significantly reduced GLUT4 expression and decreased insulin-stimulated 2-[^{3}H]deoxyglucose uptake. However, GLUT2, but not GLUT4, is the major glucose transporter in healthy hepatocytes. The similarities between molecular mechanisms regulating GLUT2 and GLUT4 translocation remain unclear. In the liver, GLUT2 regulates both glucose uptake and output (Burcelin et al., 2000; Thorens et al., 1990). Our in vitro data show that LRP1 deficiency does not affect GLUT2 protein expression. However, insulin-stimulated GLUT2 translocation from the cytosol to the plasma membrane is significantly attenuated in LRP1 deficient hepatocytes. In view of previous studies showing that loss of hepatic GLUT2 in mice suppresses hepatic glucose uptake but not secretion, leading to progressive development of glucose intolerance (Guillam et al., 1998; Seyer et al., 2013), our novel findings indicate that defective translocation of GLUT2, at least in part, accounts for impaired glucose metabolism and the development of hyperglycemia in hLRP1KO mice.

Both patients with Metabolic Syndrome and animal models of insulin resistance exhibit dyslipidemia characterized by increased plasma concentrations of VLDL-TG, low levels of HDL-cholesterol, as well as relatively normal levels of LDL cholesterol, but increased numbers of small, dense LDL particles (Choi and Ginsberg, 2011). Our data show that plasma TG levels in hLRP1KO mice are increased on chow diet, but decreased after HFD. These findings match the altered hepatic VLDL-TG secretion, but independent of the secretion of both apoB100 and apoB48. Although plasma cholesterol levels in hLRP1KO mice are reduced on chow diet, they rise to a level similar to those observed in WT mice on HFD. These findings are not paralleled by an increase of VLDL-TG. The uncoupling of cholesterol and TG secretion is also observed in liver-specific deficiency of IR (LIRKO) mice, wherein increased secretion of apoB and cholesterol is accompanied by decreased TG secretion (Biddinger et al., 2008). This highlights an important role of TG mobilization for VLDL assembly in the regulation of VLDL secretion.

The dyslipidemia in the hLRP1KO mouse model also includes increased levels of circulating NEFA, which itself is a strong predictor for insulin resistance. Although plasma NEFA levels in hLRP1KO mice are significantly higher than in WT mice, they were reduced after HFD feeding. Under fasting conditions, the plasma NEFA pool mainly originates from two sources: i) adipose tissue TG lipolyzed by adipose TG lipase (ATGL) and hormone sensitive lipase (HSL) in adipose tissue; ii) and plasma TG lipolyzed by lipoprotein lipase (LPL). Previous studies have demonstrated that LRP1 directly interacts with LPL in vitro and hepatic

LRP1 contributes to the plasma removal of catalytically inactive LPL (Espirito Santo et al., 20S04; Herz and Strickland, 2001). Additionally, in the adipose-specific LRP1 knockout mice, cell-surface LPL is elevated significantly in both WAT and brown adipose tissue (Hofmann et al., 2007). Therefore, it remains to be determined whether higher levels of adipose tissue lipolysis by lipases contribute to elevated plasma NEFA levels in hLRP1KO mice.

Along with dyslipidemia, hepatic LRP1 deficiency results in hepatic TG accumulation and severe hepatic steatosis following HFD feeding. Hepatic steatosis occurs when there is an imbalance between lipid influx (lipid delivery and de novo lipogenesis) and lipid efflux (lipid oxidation and export via VLDL) (Lee et al., 2011). Our results indicate that LRP1 deficiency is associated with lipogenesis through enhanced expression of hepatic *Scd1* and *Gpd1*. This is aggravated by HFD treatment, which leads to the activation of hepatic *Srebf1c* expression. Concurrently, the expression of genes involved in fatty acid oxidation was significantly reduced. Although the expression of most genes involved in de novo lipogenesis and FFA uptake are not affected by the absence of LRP1, inhibition or knockout of SCD1 in the liver is sufficient to protect mice from diet-induced obesity and hepatic steatosis (Jiang et al., 2005; Ntambi et al., 2002). Without any modification of the expression of *Mtp*, it is possible that augmented availability of NEFAs and subsequently more NEFA delivery to the liver could be a cause of increased VLDL-TG secretion in chow-fed hLRP1KO mice. However, in HFD-fed hLRP1KO mice with hyperinsulinemia, which itself has been shown to suppress hepatic VLDL secretion (Lee et al., 2011), excess circulating NEFA may overwhelm the capacity of the liver to unload excess TG as VLDL, leading to hepatic TG accumulation and ultimately hepatic steatosis.

Glucose intolerance and impaired insulin signaling in adipose tissue was detected only after several weeks of HFD, but not chow diet, in hLRP1-KO mice. This indicates that the HFD may progressively worsen the LRP1 deficiency-induced pure hepatic insulin resistance and further reduce insulin clearance, leading to peripheral hyperinsulinemia and insulin resistance in adipose tissues. Similarly, the hyperinsulinemia in LIRKO mice also leads to insulin resistance in fat and muscle in the absence of hypertriglyceridemia (Brown and Goldstein, 2008). In contrast to the LIRKO model, LRP1 deficiency induces a partial functional IR defect, which predisposes the mice to diet-induced insulin resistance and hepatic steatosis rather than directly triggering the development of insulin resistance, independent of a dietary stimulus.

In summary, our findings highlight the common causality of dyslipidemia, insulin resistance, and hepatic steatosis in Metabolic Syndrome. They further emphasize the physiological relevance of LRP1 for maintaining insulin sensitivity and preventing hepatic steatosis and thus underscore the central role of LRP1 as an integrator of energy homeostasis and lipoprotein metabolism.

Supplementary data to this article can be found online at http://dx.doi.org/10.1016/j.ebiom.2016.04.002.

Conflicts of Interest

The authors declare no conflicts of interest.

Author Contributions

Y.D., X.X. and J.H. designed the study. Y.D. and X.X. performed in vivo and in vitro experiments and wrote the manuscript. WL.H. performed the hyperinsulinemia-euglycemic clamp experiments. S.T. analyzed the data and performed statistical analysis. J.H. supervised the study. S.T. and J.H. reviewed and edited the manuscript.

Acknowledgements

We are indebted to Philipp Scherer for advice and helpful discussions. This work was supported by NIH grant R37 HL63762 and NS093382 (to J.H.). J.H. was supported by the American Health Assistance Foundation, the Consortium for Frontotemporal Dementia Research, the Bright Focus Foundation, the Lupe Murchison Foundation, and the Ted Nash Long Life Foundation. S.T. was supported by the American Surgical Association Foundation and the North Texas Veterans Affairs Health Care System.

References

Basford, J.E., Wancata, L., Hofmann, S.M., Silva, R.A., Davidson, W.S., Howles, P.N., Hui, D.Y., 2011. Hepatic deficiency of low density lipoprotein receptor-related protein-1 reduces high density lipoprotein secretion and plasma levels in mice. J. Biol. Chem. 286, 13079–13087.

Biddinger, S.B., Hernandez-ono, A., Rask-madsen, C., Haas, J.T., Aleman, J.O., Suzuki, R., Scapa, E.F., Agarwal, C., Carey, M.C., Stephanopoulos, G., Cohen, D.E., King, G.L., Ginsberg, H.N., Kahn, C.R., 2008. Hepatic insulin resistance is sufficient to produce dyslipidemia and susceptibility to atherosclerosis. Cell Metab. 7, 125–134.

Bilodeau, N., Fiset, A., Boulanger, M.C., Bhardwaj, S., Winstall, E., Lavoie, J.N., Faure, R.L., 2010. Proteomic analysis of Src family kinases signaling complexes in Golgi/endosomal fractions using a site-selective anti-phosphotyrosine antibody: identification of LRP1-insulin receptor complexes. J. Proteome Res. 9, 708–717.

Boucher, P., Gotthardt, M., Li, W.P., Anderson, R.G., Herz, J., 2003. LRP: role in vascular wall integrity and protection from atherosclerosis. Science 300, 329–332.

Brown, M.S., Goldstein, J.L., 2008. Selective versus total insulin resistance: a pathogenic paradox. Cell Metab. 7, 95–96.

Burcelin, R., Del carmen munoz, M., Guillam, M.T., Thorens, B., 2000. Liver hyperplasia and paradoxical regulation of glycogen metabolism and glucose-sensitive gene expression in GLUT2-null hepatocytes. Further evidence for the existence of a membrane-based glucose release pathway. J. Biol. Chem. 275, 10930–10936.

Chen, Y., Durakoglugil, M.S., Xian, X., Herz, J., 2010. ApoE4 reduces glutamate receptor function and synaptic plasticity by selectively impairing ApoE receptor recycling. Proc. Natl. Acad. Sci. U. S. A. 107, 12011–12016.

Choi, S.H., Ginsberg, H.N., 2011. Increased very low density lipoprotein (VLDL) secretion, hepatic steatosis, and insulin resistance. Trends Endocrinol. Metab. 22, 353–363.

Delgado-lista, J., Perez-martinez, P., Solivera, J., Garcia-rios, A., Perez-caballero, A.I., Lovegrove, J.A., Drevon, C.A., Defoort, C., Blaak, E.E., Dembinska-kiec, A., Riserus, U., Herruzo-gomez, E., Camargo, A., Ordovas, J.M., Roche, H., Lopez-miranda, J., 2014. Top single nucleotide polymorphisms affecting carbohydrate metabolism in metabolic syndrome: from the LIPGENE study. J. Clin. Endocrinol. Metab. 99, E384–E389.

Descamps, O., Bilheimer, D., Herz, J., 1993. Insulin stimulates receptor-mediated uptake of apoE-enriched lipoproteins and activated alpha 2-macroglobulin in adipocytes. J. Biol. Chem. 268, 974–981.

Dieckmann, M., Dietrich, M.F., Herz, J., 2010. Lipoprotein receptors—an evolutionarily ancient multifunctional receptor family. Biol. Chem. 391, 1341–1363.

Ding, Y., Zhang, L., Wang, Y., Huang, W., Tang, Y., Bai, L., Ross, C.J., Hayden, M.R., Liu, G., 2011. Amelioration of hypertriglyceridemia with hypo-alpha-cholesterolemia in LPL deficient mice by hematopoietic cell-derived LPL. PLoS One 6, e25620.

Espirito santo, S.M., Pires, N.M., Boesten, L.S., Gerritsen, G., Bovenschen, N., van Dijk, K.W., Jukema, J.W., Princen, H.M., Bensadoun, A., Li, W.P., Herz, J., Havekes, L.M., van Vlijmen, B.J., 2004. Hepatic low-density lipoprotein receptor-related protein deficiency in mice increases atherosclerosis independent of plasma cholesterol. Blood 103, 3777–3782.

Grundy, S.M., Brewer, H.B., Cleeman Jr., J.I., Smith Jr., S.C., Lenfant, C., American Heart, A., National Heart, L., Blood, I., 2004. Definition of metabolic syndrome: Report of the National Heart, Lung, and Blood Institute/American Heart Association conference on scientific issues related to definition. Circulation 109, 433–438.

Grundy, S.M., Cleeman, J.I., Daniels, S.R., Donato, K.A., Eckel, R.H., Franklin, B.A., Gordon, D.J., Krauss, R.M., Savage, P.J., Smith, S.C., Spertus Jr., J.A., Costa, F., American Heart, A., National Heart, L., Blood, I., 2005. Diagnosis and management of the metabolic syndrome: an American Heart Association/National Heart, Lung, and Blood Institute Scientific Statement. Circulation 112, 2735–2752.

Guillam, M.T., Burcelin, R., Thorens, B., 1998. Normal hepatic glucose production in the absence of GLUT2 reveals an alternative pathway for glucose release from hepatocytes. Proc. Natl. Acad. Sci. U. S. A. 95, 12317–12321.

Herz, J., Strickland, D.K., 2001. LRP: a multifunctional scavenger and signaling receptor. J. Clin. Invest. 108, 779–784.

Hofmann, S.M., Zhou, L., Perez-Tilve, D., Greer, T., Grant, E., Wancata, L., Thomas, A., Pfluger, P.T., Basford, J.E., Gilham, D., Herz, J., Tschop, M.H., Hui, D.Y., 2007. Adipocyte LDL receptor-related protein-1 expression modulates postprandial lipid transport and glucose homeostasis in mice. J. Clin. Invest. 117, 3271–3282.

Ishibashi, S., Brown, M.S., Goldstein, J.L., Gerard, R.D., Hammer, R.E., Herz, J., 1993. Hypercholesterolemia in low density lipoprotein receptor knockout mice and its reversal by adenovirus-mediated gene delivery. J. Clin. Invest. 92, 883–893.

Jedrychowski, M.P., Gartner, C.A., Gygi, S.P., Zhou, L., Herz, J., Kandror, K.V., Pilch, P.F., 2010. Proteomic analysis of GLUT4 storage vesicles reveals LRP1 to be an important vesicle component and target of insulin signaling. J. Biol. Chem. 285, 104–114.

Jiang, G., Li, Z., Liu, F., Ellsworth, K., Dallas-yang, Q., Wu, M., Ronan, J., Esau, C., Murphy, C., Szalkowski, D., Bergeron, R., Doebber, T., Zhang, B.B., 2005. Prevention of obesity in mice by antisense oligonucleotide inhibitors of stearoyl-CoA desaturase-1. J. Clin. Invest. 115, 1030–1038.

Laatsch, A., Merkel, M., Talmud, P.J., Grewal, T., Beisiegel, U., Heeren, J., 2009. Insulin stimulates hepatic low density lipoprotein receptor-related protein 1 (LRP1) to increase postprandial lipoprotein clearance. Atherosclerosis 204, 105–111.

Lee, H.Y., Birkenfeld, A.L., Jornayvaz, F.R., Jurczak, M.J., Kanda, S., Popov, V., Frederick, D.W., Zhang, D., Guigni, B., Bharadwaj, K.G., Choi, C.S., Goldberg, I.J., Park, J.H., Petersen, K.F., Samuel, V.T., Shulman, G.I., 2011. Apolipoprotein CIII overexpressing mice are predisposed to diet-induced hepatic steatosis and hepatic insulin resistance. Hepatology 54, 1650–1660.

Liu, Q., Zhang, J., Zerbinatti, C., Zhan, Y., Kolber, B.J., Herz, J., Muglia, L.J., Bu, G., 2011. Lipoprotein receptor LRP1 regulates leptin signaling and energy homeostasis in the adult central nervous system. PLoS Biol. 9, e1000575.

Liu, C.C., Hu, J., Tsai, C.W., Yue, M., Melrose, H.L., Kanekiyo, T., Bu, G., 2015. Neuronal LRP1 regulates glucose metabolism and insulin signaling in the brain. J. Neurosci. 35, 5851–5859.

Muse, E.D., Obici, S., Bhanot, S., Monia, B.P., Mckay, R.A., Rajala, M.W., Scherer, P.E., Rossetti, L., 2004. Role of resistin in diet-induced hepatic insulin resistance. J. Clin. Invest. 114, 232–239.

Ntambi, J.M., Miyazaki, M., Stoehr, J.P., Lan, H., Kendziorski, C.M., Yandell, B.S., Song, Y., Cohen, P., Friedman, J.M., Attie, A.D., 2002. Loss of stearoyl-CoA desaturase-1 function protects mice against adiposity. Proc. Natl. Acad. Sci. U. S. A. 99, 11482–11486.

Perry, R.J., Samuel, V.T., Petersen, K.F., Shulman, G.I., 2014. The role of hepatic lipids in hepatic insulin resistance and type 2 diabetes. Nature 510, 84–91.

Riccardi, G., Giacco, R., Rivellese, A.A., 2004. Dietary fat, insulin sensitivity and the metabolic syndrome. Clin. Nutr. 23, 447–456.

Rohlmann, A., Gotthardt, M., Hammer, R.E., Herz, J., 1998. Inducible inactivation of hepatic LRP gene by cre-mediated recombination confirms role of LRP in clearance of chylomicron remnants. J. Clin. Invest. 101, 689–695.

Rohlmann, A., Gotthardt, M., Willnow, T.E., Hammer, R.E., Herz, J., 1996. Sustained somatic gene inactivation by viral transfer of Cre recombinase. Nat. Biotechnol. 14, 1562–1565.

Seyer, P., Vallois, D., Poitry-Yamate, C., Schutz, F., Metref, S., Tarussio, D., Maechler, P., Staels, B., Lanz, B., Grueter, R., Decaris, J., Turner, S., Da costa, A., Preitner, F., Minehira, K., Foretz, M., Thorens, B., 2013. Hepatic glucose sensing is required to preserve beta cell glucose competence. J. Clin. Invest. 123, 1662–1676.

Takayama, Y., May, P., Anderson, R.G., Herz, J., 2005b. Low density lipoprotein receptor-related protein 1 (LRP1) controls endocytosis and c-CBL-mediated ubiquitination of the platelet-derived growth factor receptor beta (PDGFR beta). J. Biol. Chem. 280, 18504–18510.

Thorens, B., Cheng, Z.Q., Brown, D., Lodish, H.F., 1990. Liver glucose transporter: a basolateral protein in hepatocytes and intestine and kidney cells. Am. J. Phys. 259, C279–C285.

Verges, M., Bensadoun, A., Herz, J., Belcher, J.D., Havel, R.J., 2004. Endocytosis of hepatic lipase and lipoprotein lipase into rat liver hepatocytes in vivo is mediated by the low density lipoprotein receptor-related protein. J. Biol. Chem. 279, 9030–9036.

Wang, Y., Huang, Y., Hobbs, H.H., Cohen, J.C., 2012. Molecular characterization of proprotein convertase subtilisin/kexin type 9-mediated degradation of the LDLR. J. Lipid Res. 53, 1932–1943.

Xia, J.Y., Holland, W.L., Kusminski, C.M., Sun, K., Sharma, A.X., Pearson, M.J., Sifuentes, A.J., Mcdonald, J.G., Gordillo, R., Scherer, P.E., 2015. Targeted Induction of Ceramide Degradation Leads to Improved Systemic Metabolism and Reduced Hepatic Steatosis. Cell Metab. 22, 266–278.

Zhou, L., Takayama, Y., Boucher, P., Tallquist, M.D., Herz, J., 2009. LRP1 regulates architecture of the vascular wall by controlling PDGFRbeta-dependent phosphatidylinositol 3-kinase activation. PLoS One 4, e6922.